Journal of Environmental Management 297 (2021) 113223

Contents lists available at ScienceDirect

Journal of Environmental Management

journal homepage: www.elsevier.com/locate/jenvman

Incorporation of the complete ammonia oxidation (comammox) process for modeling nitrification in suspended growth wastewater treatment systems

Mohamad-Javad Mehrani, Xi Lu, Przemyslaw Kowal, Dominika Sobotka, Jacek Mąkinia *

Faculty of Civil and Environmental Engineering, Gdansk University of Technology, Ul. Narutowicza 11/12, 80-233, Gdansk, Poland

ARTICLE INFO

Keywords:
Activated sludge
Kinetic model development
Nitrification
Nitrogen removal
Wastewater treatment systems

ABSTRACT

The newly discovered process complete ammonia oxidation (comammox) has changed the traditional understanding of nitrification. In this study, three possible concepts of comammox were developed and incorporated as part of an extended two-step nitrification model. For model calibration and validation, two series of long-term biomass washout experiments were carried out at 12 °C and 20 °C in a laboratory sequencing batch reactor. The inoculum biomass was withdrawn from a large biological nutrient removal wastewater treatment plant. The efficiency of the examined models was compared based on the behaviors of ammonia, nitrite, and nitrate in the studied reactor. Predictions of the conventional approach to comammox, assuming the direct oxidation of ammonia to nitrate, were slightly better than the two other approaches. Simulation results revealed that comammox could be responsible for the conversion of >20% of the influent ammonia load. Therefore, the role of commamox in the nitrogen mass balance in activated sludge systems should not be neglected and requires further investigation. Furthermore, sensitivity and correlation analysis revealed that the maximum growth rates (μ), oxygen half-saturation (K_O), and decay rates (b) of the canonical nitrifiers and comammox were the most sensitive factors, and the highest correlation was found between μ and b among all considered kinetic parameters. The estimated μ values by the best model were 0.57, 0.11, and 0.15 d^{-1} for AOB, NOB, and comammox bacteria, respectively.

1. Introduction

Nitrification is a vital process for effective nitrogen (N) removal in wastewater treatment plants (WWTPs). Traditionally, that process has been assumed to consist of two consecutive steps, including ammonia oxidation to nitrite by ammonia oxidizing bacteria (AOB), followed by nitrite oxidation to nitrate by nitrite oxidizing bacteria (NOB) (Jaramillo et al., 2018; Noriega-Hevia et al., 2020). However, the recently discovered complete ammonia oxidation (comammox) process has changed the dogma of the strict two-step nitrification (Daims et al., 2015; van Kessel et al., 2015).

Comammox is a process of converting ammonia directly to nitrate by a single microorganism belonging to *Nitrospira*, further referred to as comammox *Nitrospira*. In comparison with canonical NOB, comammox *Nitrospira* possesses genes related to both ammonia oxidation and nitrite oxidation (Lawson and Lücker, 2018). This unique metabolic pathway makes comammox bacteria different from other canonical nitrifiers (Palomo et al., 2018; Annavajhala et al., 2018).

There has been some evidence that comammox bacteria are not able to compete with other nitrifiers (AOB, NOB) in wastewater treatment systems (Annavajhala et al., 2018; Gonzalez-Martinez et al., 2016). In contrast, comammox *Nitrospira* were found to be dominant in comparison with either AOB (Roots et al., 2019) or NOB (Sun et al., 2018; Zhou et al., 2018) in nitrifying activated sludge systems. The potentially favorable conditions for the growth of comammox *Nitrospira* comprise either low dissolved oxygen (DO) and ammonia concentrations (Palomo et al., 2018; Roots et al., 2019) or a nitrite-limited environment (Park et al., 2017) with long solids retention times (SRTs) (Qian et al., 2017). The competition for ammonia (NH_4–N) between canonical AOB and comammox microorganisms could play a vital role in achieving partial nitrification (nitritation), which is required in shortcut N removal processes, such as “nitrite shunt” or deammonification (Izadi et al., 2021).

Simulation models are an important management tool in the operation of WWTPs and help in understanding the complex microbial interactions in biological wastewater treatment systems (Metcalf and Eddy, 2014). Nitrification is an inherent part of activated sludge models (ASMs). For simplicity, the full nitrification pathway, i.e., oxidation of ammonia to nitrate, has traditionally been modeled as a single-step

* Corresponding author. Gdansk University of Technology, Ul. Narutowicza 11/12, 80-233, Gdansk, Poland.
E-mail address: jmakinia@pg.edu.pl (J. Mąkinia).

https://doi.org/10.1016/j.jenvman.2021.113223
Received 6 March 2021; Received in revised form 1 July 2021; Accepted 2 July 2021

process assuming that the first step (ammonia oxidation to nitrite) is typically the rate-limiting conversion in the entire oxidation pathway. This approach has been adopted in all the most common complex activated sludge models (ASMs), including the IWA ASM series (Henze, 2000). Two-step nitrification models have been known and continuously developed for almost 60 years as summarized by (Makinia and Zaborowska, 2020). However, those models became particularly important when nitrite received growing attention as the central component in the shortcut N removal processes.

Cao et al. (2017) noted that the nitrification models should appropriately accommodate the competition between AOB and NOB to understand factors influencing the competition between autotrophic N-converting organisms. Multistep nitrification models also incorporate AOB-mediated pathways of N_2O production pathways via hydroxylamine production or/and autotrophic denitrification (Domingo-Félez and Smets, 2016). An ASM3 model was applied for optimization and simulation of chemical oxygen demand (COD) and ammonia removal from coking wastewater treatment plants (WWTPs) by (Wu et al., 2016), and very recently, Karlikanovaite-Balikci and Yagci (2019) determined the characteristics of a sludge reduction process by calibration of kinetic parameters using modified ASM1. Additionally (Yu et al., 2020), expanded the traditional two-step nitrification model and incorporated different species of AOB (*Nitrosomonas* vs. *Nitrosospira*) and NOB (*Nitrobacter* vs. *Nitrospira*) based on the r/K theory assumptions.

Despite the fast-growing number of experimental studies on comammox, the process has not yet been considered for expansion of nitrification models. The present study aimed to (1) evaluate the capabilities and limits of three novel model concepts for the comammox process, (2) predict the coexistence of comammox and canonical AOB and NOB under highly dynamic conditions during biomass washout experiments, and (3) evaluate the role of comammox in ammonia conversion to nitrate. The models were calibrated and validated with experimental data from a laboratory-scale sequencing batch reactor (SBR) with inoculum biomass from a full-scale WWTP. Sensitivity analysis and correlation matrix analysis were performed to identify kinetic parameters that were most influential for predictions of the expanded models. It was hypothesized that the newly developed mechanistic models could reveal the potential role of comammox in nitrifying systems and enhance the current understanding of N conversions in those systems.

2. Materials and methods

2.1. Conceptual and mathematical model description

Even though it is well established that comammox is a two-step process and comammox Nitrospira possesses key enzymes for both NH_4–N and NO_2–N oxidation. However, there is no consensus in the literature if NO_2–N is released outside of the cells during the process. Daims et al. (2016) hypothesized and Wu et al. (2019) experimentally demonstrated that NO_2–N could be an intracellular transit product of comammox. On the other hand, transient NO_2–N accumulation produced by comammox Nitrospira during NH_4–N oxidation has also been reported (Kits et al., 2017; Ren et al., 2020). Furthermore, Koch et al. (2019) noted that in contrast to canonical NOB, currently cultivable comammox Nitrospira species cannot grow under NO_2–N only conditions. Other authors did not exclude that comammox bacteria could use NO_2–N as electron donors when NH_4–N is temporarily unavailable (Kits et al., 2017; Palomo et al., 2018; Roots et al., 2019). In a very recent study, Sun et al. (2018) have noted that the comammox species reveal variable nitrite affinities.

The current study attempted to differentiate between the potential mechanisms of the comammox process in converting NH_4–N to NO_3–N. Three different nitrification model concepts, including comammox, are presented in Fig. 1. A mathematical notation of those models, including their stoichiometric matrices and vectors of kinetic expressions, is presented in Table S1 in the Supplementary Information (SI).

In Model I, the complete NH_4–N oxidation is assumed to be a one-step process (NH_4–N→NO_3–N) without release of extracellular NO_2–N, and comammox bacteria are not able to utilize extracellular NO_2–N as electron donors. In Model II and Model III, comammox bacteria are assumed to be able to utilize extracellular NO_2–N as the electron donors. The difference between those two models is that NH_4–N and NO_2–N oxidation is modeled as either a sequential two-step process (NH_4–N→NO_2–N→NO_3–N) in Model II or a hybrid process in Model III, e.g., NH_4–N→NO_3–N (similar to Model I) and NO_2–N→NO_3–N (similar to Model II). However, the latter process is activated by a switching function, when the availability of NH_4–N becomes limited.

2.2. Stoichiometric and kinetic parameters

An overview of recent literature data on stoichiometric and kinetic parameters for canonical AOB, canonical NOB, and comammox bacteria is presented in Table S2 in the SI. In terms of r/K selection theory, canonical nitrifiers can be categorized into the fast-growing (r-strategists) and the slow-growing (K-strategists) bacteria. These differences result from the operational conditions, sludge floc morphology, and cultivation environment (Yu et al., 2020). Comammox *Nitrospira* may have a higher growth yield compared to other canonical AOB and NOB in addition to the key characteristics of canonical AOB, including a high ammonia affinity and a low maximum specific growth rate (Kits et al., 2017). Moreover, Koch et al. (2019) reported that two distinct clades (A and B) were found within comammox *Nitrospira*, showing similar ammonium affinities to either AOB or canonical *Nitrospira*.

2.3. Modeling and simulation platform

The GPS-X (Hydromantis, Canada) (www.hydromantis.com) is an

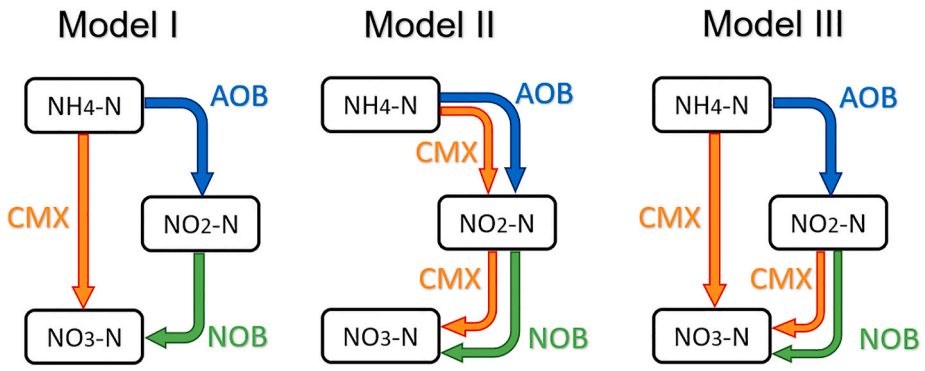

Fig. 1. Three conceptual models of comammox as an extension of the two-step nitrification pathways (microorganisms responsible for the specific processes are AOB (nitritation), NOB (nitratation), and CMX (comammox).

open modeling and simulation platform for various wastewater treatment processes. Some of the useful features were used in the present study, including the following:

- ***Model Developer (MD)***, which allows for the writing of new models and modification of existing models (stoichiometric matrix and vector of kinetic rate expressions).
- ***Sensitivity Analyzer***, which performs steady-state, phase dynamic, or time dynamic simulations for selected intervals of any independent variable.
- ***Parameter Optimizer***, which uses the Nelder-Mead simplex method with one of five different objective functions to search for the parameter values with the minimum variance between measured data and model predictions.

2.4. Experimental data for model calibration and validation

2.4.1. Biomass washout experiments in a sequencing batch reactor

Washout experiments aim at washing out specific groups of microorganisms (most often NOB) from a system by applying specific operational conditions. In this study, long-term biomass cultivations were conducted at decreasing SRTs. The inoculum biomass for two experiments was withdrawn in the winter and summer seasons from the "Czajka" WWTP in Warsaw. These experiments were carried out in an SBR with a working volume of 10 L. In both cases, the reactor was operated for 30 days at 12 °C (experiment 1) and 20 °C (experiment 2). Air was supplied in a continuous aeration mode, the DO set point was 0.6 ± 0.1 mg O_2/L, and the pH was kept at 7.5 for both experiments.

A single operational cycle lasted 480 min and consisted of three phases: feeding (15 min), reaction (450 min), and decanting (15 min). The SRT gradually decreased from 4 d to approximately 1 d. The reduced SRT and low DO concentration were combined factors to evaluate the suppression of NOB in the SBR. The initial mixed liquor suspended solids (MLSS) concentration and its volatile fraction (MLVSS) were approximately 2000 mg/L and 1300 mg/L at 12 °C, and 2500 mg/L, 1500 mg/L for 20 °C, respectively. The SBR was fed ammonium-rich synthetic medium with tracer elements. The volumetric nitrogen loading rates (NLRs) were generally kept at approximately 0.02 ± 0.01 g N/(L·d) and 0.05 ± 0.01 g N/(L·d) during the 12 °C and 20 °C experiments, respectively.

2.4.2. Short-term batch experiments

Before the long-term washout experiments in the SBR, two series of short-term batch experiments were carried out with mixed liquor from the Czajka WWTP. These experiments aimed to estimate kinetic parameters (half-saturation constants – $K_{O,AOB}$, $K_{O,NOB}$, $K_{NO2,NOB}$) for the two-step nitrification model. The kinetic parameters were estimated after linearization of the Monod equation as described in detail in the SI. The tests were carried out at seven DO concentrations (0.2, 0.5, 0.7, 1.0, 1.5, 2.0, 2.5 mg O_2/L) under winter (12 °C) and summer (20 °C) conditions. The substrate was a synthetic medium containing either ammonium (NH_4Cl) or nitrite ($NaNO_2$) with supplemental sodium bicarbonate ($NaHCO_3$) as an inorganic carbon source. In both cases, the initial concentration of the substrate was approximately 20 mg N/L. The pH was kept at 7.5 by dosing NaOH (2 M solution).

2.5. Initial biomass concentration and composition

The initial shares of AOB, NOB and coammox bacteria for modeling were determined in two steps. First, since the exact operating data were not available at the studied plant, the overall nitrifier concentration was assumed based on the previous results of stead-state and dynamic simulations of two similar large WWTPs in Poland (Makinia et al., 2006). The predicted concentrations ranged from 38 to 62 mg COD/L which was on average approximately 2% of the particulate COD in the studied WWTPs. In the second step, the relative distributions of AOB, canonical NOB, and comammox bacteria were estimated from microbial analysis using a combined approach of 16 S rRNA gene high-throughput sequencing technique and quantitative PCR (qPCR), which were described in detail elsewhere (Kowal et al., 2021). For simulations, the average initial ratios of AOB:NOB:comammox bacteria were set at 3:9:1 for both experiments. This assumption was made based on the observation of similar trends of NH_4–N, NO_2–N and NO_3–N during both washout experiments. It should be emphasized that the total nitrifier abundance and AOB:NOB proportions were within the ranges reported by (Griffin and Wells, 2017) for six full-scale bioreactors.

2.6. Model implementation, calibration, validation, and comparison

The three mathematical models, described in section 2.1, were implemented in GPS-X using the MD utility and the ASM1 (Henze et al., 2000) as the core model. The nitrification process was expanded from one stage into two separate stages (AOB and NOB) and the comammox kinetics and stoichiometry were defined. Sensitivity analysis was performed to select the most sensitive parameters related to the nitrification process. Pairs of the highly correlated parameters were identified based on the correlation matrix results.

Calibration and validation are critical steps in the modeling process that address the model prediction capability and its reliability of use under different conditions. Therefore, in the present study, each examined model was calibrated with the same measurement data (NH_4–N, NO_2–N, NO_3–N) from the experiment carried out at 12 °C. The influential and noncorrelated parameters were estimated using the GPS-X "optimizer" utility. The estimation process was conducted until the maximum sizes for all of the parameter dimensions decreased below the parameter tolerance (Lu et al., 2018). Moreover, the 95% confidence limits for each parameter estimate were calculated from the variance-covariance matrix.

Subsequently, the models were validated with another set of experimental data from the experiment carried out at 20 °C. In addition, the comammox influence on the model predictions was evaluated by setting the values of μ_{CMX} and b_{CMX} to 0. The entire modeling/simulation procedure is presented in Fig. 2 and the most important steps are described in the following sections.

Although the operational conditions were unfavorable for denitrification (there was no organic carbon in the feed and reactor aeration), that process was still considered in modeling but without further adjustments of the model default parameters.

2.6.1. Local sensitivity analysis

Local sensitivity analysis (LSA) is a method in which one or more uncertain variables are selected to determine their influence on some results or quantities of importance in mathematical models (Hong et al., 2019; Razavi et al., 2021). In the present study, a local one-variable-at-a-time sensitivity analysis was carried out for 13 kinetic parameters targeting the N components, such as NH_4–N, NO_2–N, and NO_3–N concentrations. The initial values for the examined kinetic parameters are presented in Table 1. Simulations were run under dynamic conditions using a GPS-X "phase dynamic" sensitivity analyzer. Similar to (Lu et al., 2018), an uncertainty of 20% (±10% of the adjusted value) was allocated to each considered parameter. The normalized sensitivity coefficient ($S_{i,j}$) was defined as the ratio of the percentage change ($\Delta y_{i,j}/y_i$) in the *i-th* output variable (y_i) to the percentage change ($\Delta x_j/x_j$) in the *j-th* model parameter (x_j):

$$S_{i,j} = \left| \frac{\Delta y_{i,j}}{y_i} \cdot \frac{x_j}{\Delta x_j} \right| \quad (1)$$

The influence of each adjusted parameter on the specific model output was defined using the following classification (Lu et al., 2018): 1) insignificantly influential ($S_{i,j} < 0.25$), 2) influential ($0.25 \leq S_{i,j} < 1$), 3) very influential ($1 \leq S_{i,j} < 2$), and 4) extremely influential ($S_{i,j} \geq 2$).

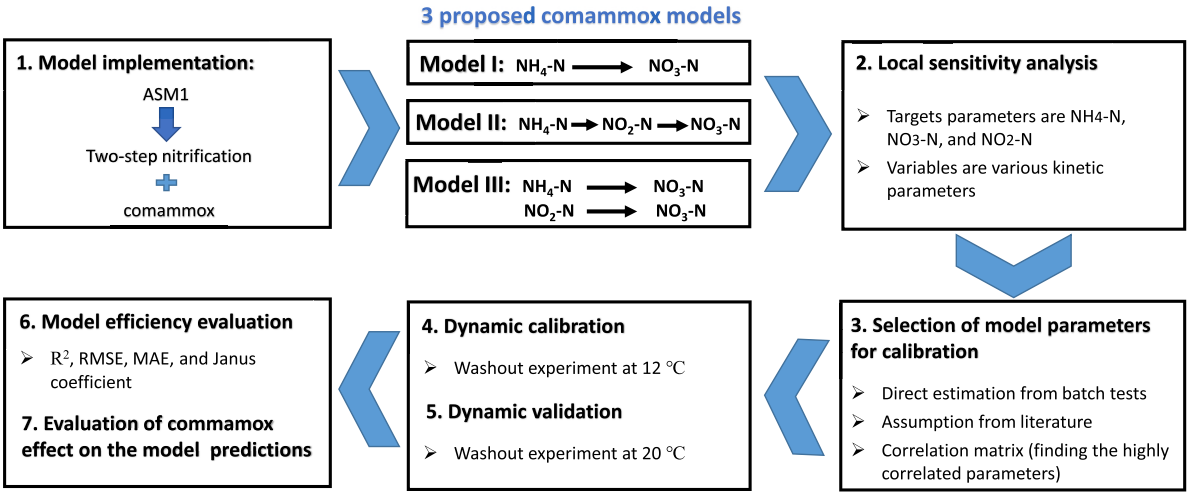

Fig. 2. The procedure of the implementation, calibration, validation, and comparison of the expanded nitrification models including comammox.

Table 1
Initial values of the kinetic parameters selected for sensitivity analysis of the models.

Bacteria	Kinetic parameter	Unit	Initial values	Reference
AOB	μ_{AOB}	d^{-1}	1.01	Yu et al. (2020)
	$K_{NH4,AOB}$	mg N/L	0.675	Yu et al. (2020)
	$K_{O,AOB}$	mg O_2/L	0.30	Batch test
	b_{AOB}	d^{-1}	0.15	Yu et al. (2020)
NOB	μ_{NOB}	d^{-1}	0.31	Yu et al. (2020)
	$K_{NO2,NOB}$	mg N/L	0.057	Batch test
	$K_{O,NOB}$	mg O_2/L	0.2	Batch test
	b_{NOB}	d^{-1}	0.05	Yu et al. (2020)
CMX	μ_{CMX}	d^{-1}	0.69	Park et al. (2017)
	$K_{NH4,CMX}$	mg N/L	0.01	Koch et al. (2019)
	$K_{NO2,CMX}$	mg N/L	6.29	Koch et al. (2019)
	$K_{O,CMX}$	mg O_2/L	0.33	Park et al. (2017)
	b_{CMX}[a]	d^{-1}	0.05	Yu et al. (2020)

[a] no reference available yet (the assumed value is the same as that for NOB).

2.6.2. Selection of the kinetic parameters for optimization in GPS-X

Two groups of kinetic parameters were excluded from the selection for optimization in GPS-X:

- Least influential parameters determined based on the LSA results.
- Three important kinetic parameters, including the oxygen half-saturation constants for AOB and NOB ($K_{O,AOB}$, $K_{O,NOB}$), and nitrite half-saturation constants for NOB ($K_{NO2,NOB}$) were determined directly based on the preliminary batch experiments (section 2.4.2). A detailed description of the calculations can be found in the SI.

Subsequently, the correlation matrix was developed to evaluate the linear relationship, its strength, and direction (positive vs. negative) for pairs of influential model parameters. If the obtained correlation coefficient is strong enough for any parameter pair, then the calibration process can be simplified by fixing one of the parameters (Zhu et al., 2015). Cao et al. (2020) defined the correlations as strong, moderate, and weak when the coefficients were >0.68, 0.36–0.68, and <0.36, respectively. This classification was adopted in the present study.

2.6.3. Comparison of model efficiencies

To examine the model efficiency (goodness-of-fit), diverse evaluation measures can be used (Hauduc et al., 2015). The most common ones, implemented in GPS-X, include the determination coefficient (R^2), root mean square error (RMSE), and mean absolute error (MAE). The RMSE quantifies the global error of the model while keeping the same unit as the target variable, whereas the MAE evaluates the quality of an estimated parameter in terms of its variation and unbiasedness (Hauduc et al., 2015). In addition, the Janus coefficient (J^2) was calculated in the present study. The J^2 coefficient does not evaluate the model efficiency, but it indicates a change in the model efficiency between the calibration and validation steps. When J^2 is close to 1, the model performance is similar in both steps (the model is valid), whereas high J^2 values could indicate a lack of model robustness.

3. Results and discussion

3.1. Local sensitivity analysis

Fig. 3 shows the sensitivity coefficients for all 13 kinetic parameters related to AOB, NOB, and comammox bacteria in the three examined model structures (Models I, II, and III). The extremely influential parameters (2 parameters with $S_{i,j} \geq 2$) occurred only in Model I, but the highest number of the influential parameters (6 parameters with $S_{i,j} \geq 1$) occurred in Model II.

For all three model structures, the maximum specific growth rate of AOB (μ_{AOB}) was the most influential parameter concerning the behavior of both nitritation substrate (NH_4–N) and product (NO_2^-N), with $S_{i,j}$ ranges of approximately 1.0–1.5 and 1.1–2.3, respectively. The oxygen half-saturation coefficient for AOB ($K_{O,AOB}$) and decay coefficient for AOB (b_{AOB}) were very influential on the behavior of NO_2^-N, with $S_{i,j}$ ranges of approximately 0.9–1.8 ($K_{O,AOB}$) and 1.3–1.6 (b_{AOB}). These two parameters were still very influential in Models I and III with respect to the behavior of NH_4–N. The parameters related to the NOB kinetics, i.e. the maximum specific growth rate (μ_{NOB}) and oxygen half-saturation constant ($K_{O,NOB}$), were at least influential ($S_{i,j} > 0.25$) on the behavior of both nitratation substrate (NO_2^-N) and product (NO_3–N).

The influence of the parameters related to the comammox kinetics varied among the examined models. For Model I, the maximum specific growth rate of comammox bacteria (μ_{CMX}) was extremely influential with respect only to NO_3^-N (comammox product), with the highest sensitivity coefficient among all the models ($S_{i,j} = 2.47$). The oxygen half-saturation coefficient ($K_{O,CMX}$) and decay coefficient (b_{CMX}) for comammox bacteria were very influential only on the behavior of NO_3^-N, with $S_{i,j}$ of approximately 1.4 for both parameters. For Models II and III, μ_{CMX} was very influential on the behavior of NO_2–N ($S_{i,j} \approx$ 1.3–1.4) and NO_3–N ($S_{i,j} \approx$ 0.8–1.6). Moreover, for Model III, b_{CMX} had the highest influence ($S_{i,j} = 0.87$) on NO_3–N among all the kinetic parameters.

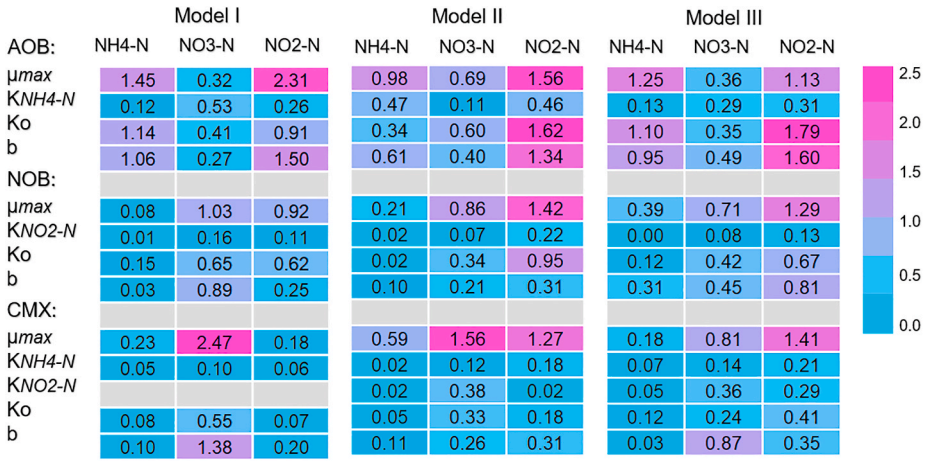

Fig. 3. Heatmap of the sensitivity coefficients for the three examined models.

3.2. Values of the kinetic parameters

For simulations, the kinetic parameter values were selected using three approaches: literature data, direct determination from the batch experiments, and mathematical optimization (estimation) (Table 2). Based on the sensitivity analysis results, values for the least influential parameters, including the half-saturation coefficients for AOB ($K_{NH4,AOB}$) and comammox bacteria ($K_{NH4,CMX}$, $K_{NO2,CMX}$), were adopted from the literature (Koch et al., 2019; Park et al., 2017; Yu et al., 2020) as shown in Table S2 in SI.

The values of DO half-saturation coefficients for AOB ($K_{O,AOB}$) and NOB ($K_{O,NOB}$) and the nitrite half-saturation coefficient for NOB ($K_{NO2,NOB}$) were determined from the batch experiments as described in the SI. Three different linearized forms of the Monod equation and the least-square method were used. In all cases, the highest determination coefficient ($R^2 > 0.9$) was obtained for the Hanes equation.

The values of $K_{O,AOB} = 0.3$ mg O_2/L and $K_{O,NOB} = 0.2$ mg O_2/L were within the literature ranges of 0.16–1.22 mg O_2/L (Zhang et al., 2019) and 0.17–4.32 mg O_2/L (Park et al., 2017), respectively. The value of $K_{NO2-N} = 0.057$ mg N/L was slightly below the ranges reported by (Park et al., 2017) and Koch et al. (2019) for canonical K–NOB (Table 2). Furthermore, a comparison of the process rates at 12 °C and 20 °C suggested that the temperature correction factors in the Arrhenius equation for AOB and NOB were approximately 1.11 (see: SI for details). This value has commonly been used in activated sludge modeling studies (Henze et al., 2000). The most influential parameters (μ_{AOB}, μ_{NOB}, μ_{CMX}, $K_{O,AOB}$, $K_{O,NOB}$, $K_{O,CMX}$, and b_{AOB}, b_{NOB}, b_{CMX}) were selected for evaluation in the correlation matrix before mathematical optimization using the GPS-X "Optimizer" utility.

3.3. Correlation matrix

Fig. 4 shows the overall correlation matrix developed for the most influential kinetic parameters. In the case of all the nitrifier groups, the DO half-saturation constants (Ko) revealed a strong correlation with the maximum specific growth rates (μ) in the three examined models. Therefore, the K_O coefficients were excluded from the optimization process and their values were either determined from the batch test results ($K_{O,AOB}$ and $K_{O,NOB}$) or adopted from the literature ($K_{O,CMX}$).

In general, the highest values of the correlation coefficient referred to the relationship of μ_{AOB}, μ_{NOB}, and μ_{CMX} with the corresponding decay coefficients (b_{AOB}, b_{NOB} and b_{CMX}) in all three models. At short SRTs, as in the present study, attention is normally directed towards growth rather than decay kinetics. Hence, only the maximum specific growth rates were selected for the further optimization process, while the default values of b coefficients were assumed for simulations. However, the accurate estimation of b coefficients becomes more important with increasing SRT (Dold et al., 2005).

The other pairs of highly correlated parameters comprised μ_{AOB} with μ_{NOB} (0.62–0.71), and $K_{O,AOB}$ with $K_{O,NOB}$ (0.66–0.74). High correlations (0.71–0.74) were also found in specific models between b_{AOB} and μ_{AOB} (Model III), μ_{AOB} and μ_{NOB} (Model III) as well as $K_{O,AOB}$ and $K_{O,NOB}$ (Model I).

Table 2
Methods of selection of kinetic parameters and their values in the three examined models.

Bacteria	Kinetic parameter	Unit	Initial value	Calibration results			Source		
				Model I	Model II	Model III	Literature	Batch tests	Calibration
AOB	μ_{AOB}	d^{-1}	1.01	0.57	0.55	0.60			×
	$K_{NH4,AOB}$	mg N/L	0.675	0.675	0.675	0.675	×		
	$K_{O,AOB}$	mg O_2/L	0.30	0.30	0.30	0.30		×	
	b_{AOB}	d^{-1}	0.15	0.15	0.15	0.15	×		
NOB	μ_{NOB}	d^{-1}	0.31	0.11	0.11	0.11			×
	$K_{NO2,NOB}$	mg N/L	0.057	0.057	0.057	0.057		×	
	$K_{O,NOB}$	mg O_2/L	0.2	0.2	0.2	0.2		×	
	b_{NOB}	d^{-1}	0.05	0.05	0.05	0.05	×		
CMX	μ_{CMX}	d^{-1}	0.69	0.15	0.20	0.22			×
	$K_{NH4,CMX}$	mg N/L	0.01	0.01	0.01	0.01	×		
	$K_{NO2,CMX}$	mg N/L	6.29	0.0[a]	6.29	6.29	×		
	$K_{O,CMX}$	mg O_2/L	0.33	0.33	0.33	0.33	×		
	b_{CMX}	d^{-1}	0.05	0.05	0.05	0.05	×		

μ: maximum specific grow rate, K: half-saturation coefficient, b: decay coefficient.
[a] Model I does not use nitrite as a substrate in comammox process.

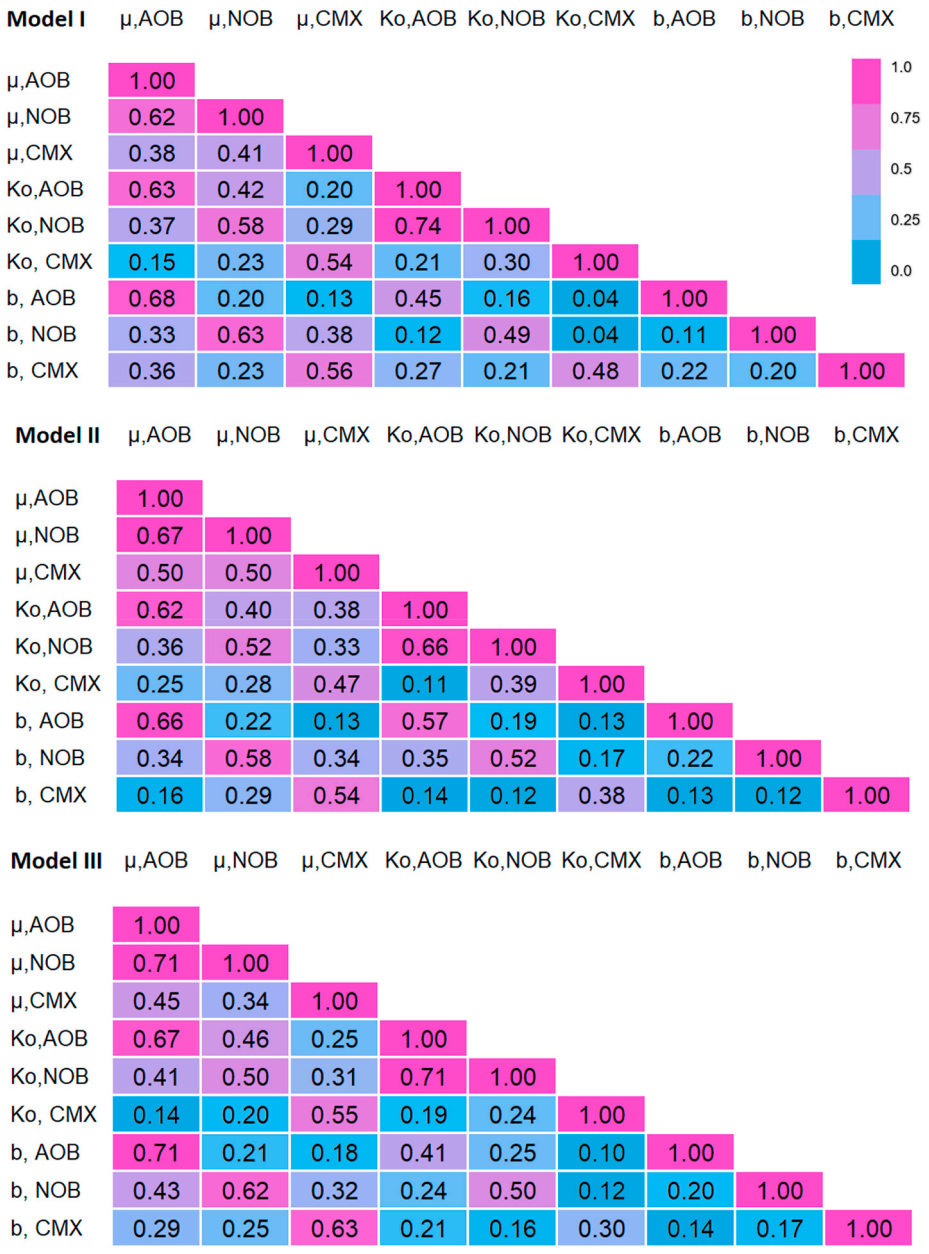

Fig. 4. Correlation matrix of the adjusted kinetic parameters.

3.4. Model calibration (parameter estimation)

In the first step, the predicted biomass concentrations (MLSS and MLVSS) were checked against the measurements at 12 °C for each model as shown in Fig. 5a. The initial measured MLSS concentration was approximately 1950 mg/L and it decreased below 300 mg/L at the end of the experiment. The nitrifier population was subjected to great dynamics under specific operational conditions, resulting from aggressive SRT reduction. Fig. 5b shows the predicted biomass concentrations of the specific groups of nitrifiers. Their predicted ultimate washout was confirmed by microbiological analyses using a combination of 16 S rRNA high-throughput sequencing and qPCR techniques (Kowal et al., 2021).

The observed and predicted behaviors of NH_4–N, NO_3–N, and NO_2–N are shown in Fig. 6. The prediction accuracy of each model for the three N components was individually interpreted by plotting the model predictions vs. measured data, as shown in Fig. 7. Numerical values of all the model efficiency measures (R^2, RMSE, MAE) are listed in Table 3. From the comparative results of the calibrated models, it appears that the best goodness-of-fit was obtained for Model I. That model revealed the highest R^2 values of 0.96, 0.92, and 0.93 for NH_4–N, NO_3–N, and NO_2–N, respectively. Moreover, the RMSE and MAE were also lower than those of the other two models.

When comparing the values of model parameters adjusted during calibration (Table 2), it appears that there were only slight changes in μ_{AOB} and μ_{NOB} between the models. The optimized values of 0.55–0.60 d^{-1} (μ_{AOB}) and 0.11 d^{-1} (μ_{NOB}) are within the ranges reported in other studies (Park et al., 2017; Zhang et al., 2019) (Table S2). In addition, low variances were observed between the examined models for μ_{CMX} (0.15–0.22 d^{-1}), which resulted from the number of substrates for comammox bacteria. In the model (Model I) with a single substrate (NH_4–N), $\mu_{CMX} = 0.15\ d^{-1}$ was lower than $\mu_{CMX} = 0.2$–$0.22\ d^{-1}$ in the models with two substrates (Model II and Model III). In this way, the overall growth rates of comammox bacteria became comparable.

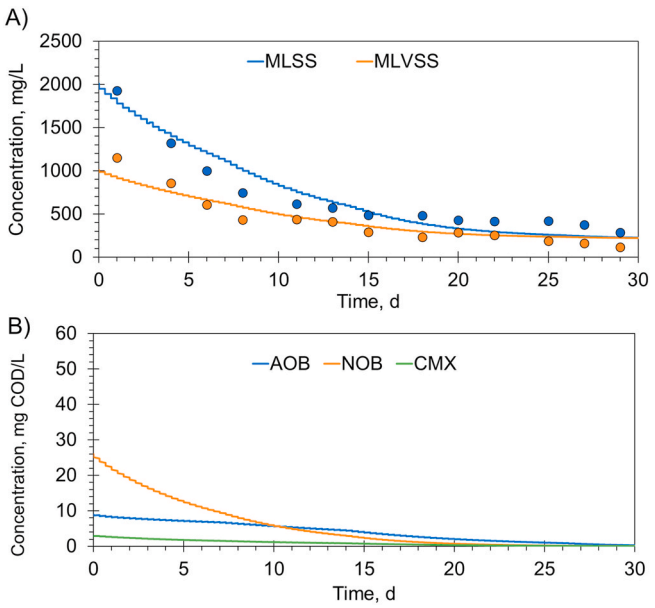

Fig. 5. Measured and predicted MLSS and MLVSS concentrations (A) and predicted active biomass concentrations of specific nitrifiers (AOB, NOB and CMX) (B) during the calibration phase.

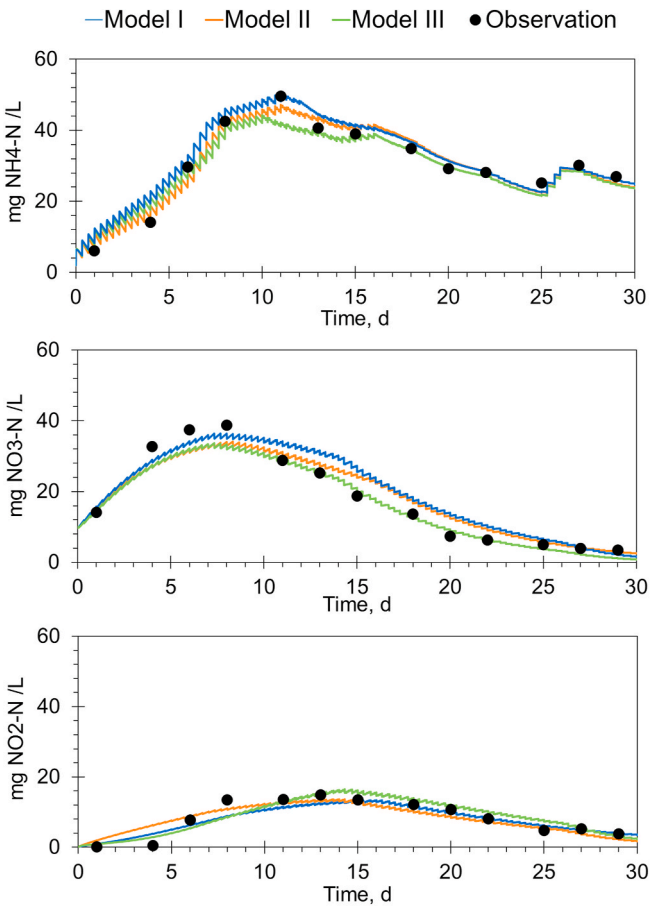

Fig. 6. Measured data vs. model predictions of NH_4–N, NO_2–N, and NO_3–N in Models I, II and III (calibration phase).

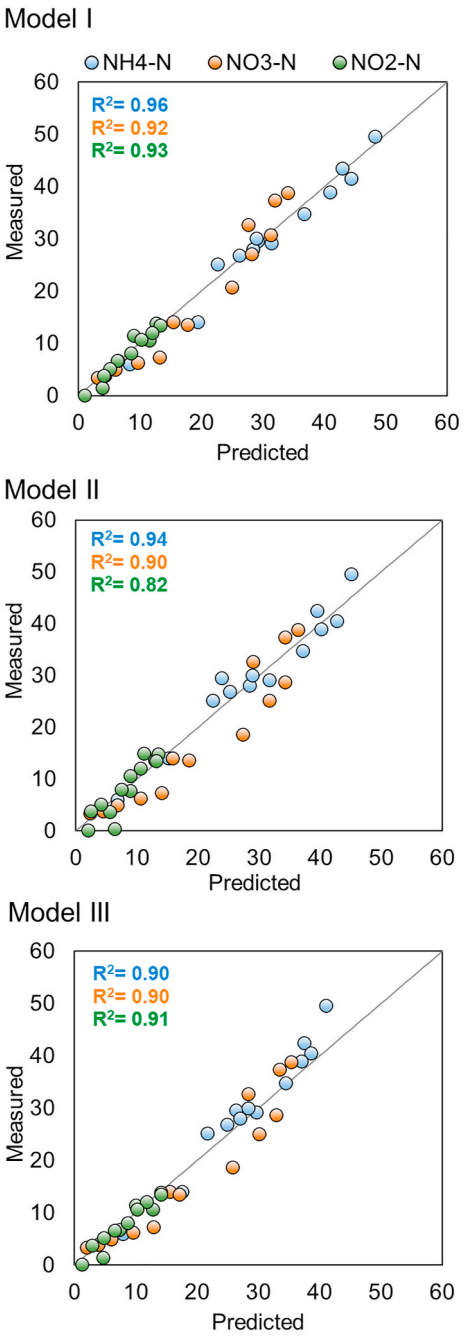

Fig. 7. Correlation between the observed data and model predictions of each examined model for the different N components.

3.5. Model validation

For model validation, predictions of the examined models were compared with the data from the washout experiment carried out at 20 °C. The observed and predicted behaviors of biomass (MLSS, MLVSS), NH_4–N, NO_3–N, and NO_2–N are shown in the SI (Figs. S5 and S6). The summarized information on the efficiency of the validated models is presented in Table 3. Overall, the validation results in terms of R^2, RMSE, and MAE confirm the reliability and robustness of the models despite different conceptual formulations of the commamox process. In addition, the Janus coefficient (J^2) was calculated to compare the goodness-of-fits in the calibration and validation phases. For Model III, the closest value to 1.0 was obtained, but the J^2 values for the other models were only slightly higher (Table 3). Therefore, all models are

Table 3
Summarized information on the model efficiency during the calibration and validation periods.

Model	State variables	Calibration phase			Validation phase			
		R^2	RMSE	MAE	R^2	RMSE	MAE	J^2
I	NH_4–N	0.96	1.84	1.91	0.76	2.90	4.75	2.48
	NO_3–N	0.92	2.08	2.13	0.88	3.10	4.18	2.22
	NO_2–N	0.93	2.13	2.28	0.64	4.23	5.24	3.76
II	NH_4–N	0.94	2.07	2.73	0.79	3.45	5.71	2.77
	NO_3–N	0.90	2.15	3.46	0.84	4.12	5.05	3.67
	NO_2–N	0.82	2.94	3.41	0.61	5.46	6.84	3.44
III	NH_4–N	0.90	2.13	3.72	0.80	3.30	5.50	2.40
	NO_3–N	0.90	2.89	4.31	0.86	3.10	4.25	1.15
	NO_2–N	0.91	2.25	3.01	0.79	3.140	4.30	1.94

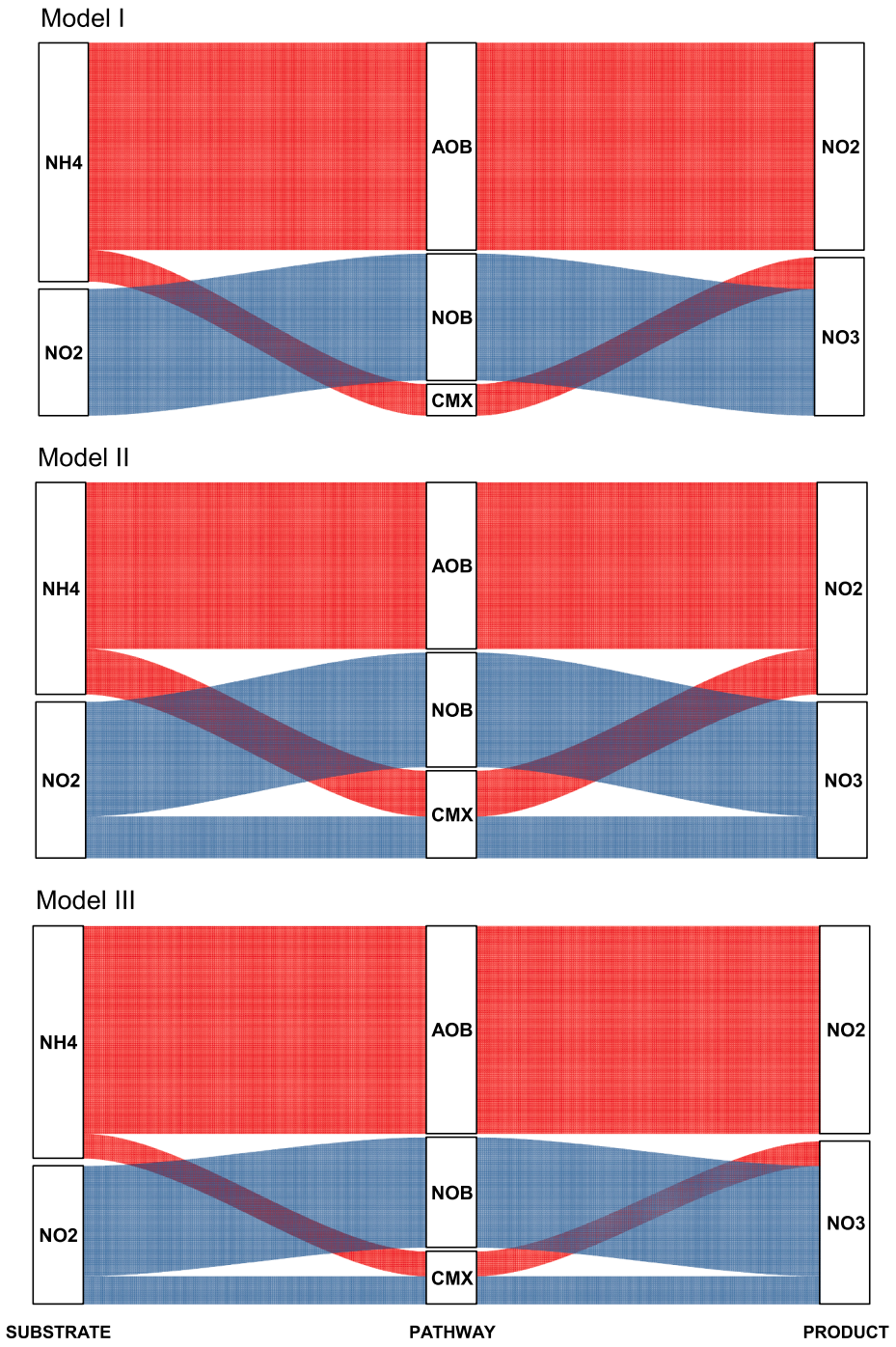

Fig. 8. Sankey graphs of the nitrogen conversions during the calibration phase (developed based on the average values during the entire calibration period).

valid in terms of Janus coefficient evaluation.

From the conceptual point of view, Model I was simplest among the examined models and its efficiency was only slightly better than the others under specific operational conditions (solely NH_4–N in the feed). However, Model I could be replaced with Model III when it was confirmed that NO_2–N is indeed a substrate for comammox bacteria.

3.6. Effect of commamox on the model predictions

To evaluate of comammox effect on the calibration process, two-step nitrification models were run without the comammox activity (μ_{CMX} and b_{CMX} set to 0) and the results are shown in the SI (Fig. S7).

The nitrogen conversion pathways in the examined models were also analyzed using Sankey graphs (Fig. 8) based on the average values for the entire calibration period (30 d). The predicted contribution of comammox bacteria was notable but less significant than that of canonical nitrifiers.

When the direct oxidation of NH_4–N to NO_3–N by comammox bacteria was considered (Models I and III), that pathway was responsible for the conversion of 14% (Model I) and 11% (Model III) of NH_4–N compared to 86% and 89%, respectively, oxidized to NO_2–N by AOB. In Model II considering the parallel oxidation of NH_4–N to NO_2–N by AOB and comammox bacteria, 21% of NH_4–N was oxidized by comammox bacteria and the remaining 79% was converted by AOB. When oxidation of NO_2–N to NO_3–N by comammox bacteria was considered (Models II and III), that pathway was also less significant than the oxidation by NOB. The contributions of commamox bacteria were 26% and 20% in Model II and Model III, respectively, with the remaining contributions of NOB.

4. Conclusions

Different comammox model concepts may be integrated with the existing two-step nitrification models while obtaining a similar predictive performance. The model efficiency measures (R^2, RMSE, MAE) for the approach assuming the direct oxidation of NH_4^+-N to NO_3^--N (without the use of NO_2^--N as an external substrate), were only slightly better than those of the other possible approaches. The model preference could be established after confirming the actual mechanism of NO_2^--N and determining the key model parameters for comammox.

Even though the maximum specific growth rate of comammox bacteria was variable between the examined models, its value remained in the same order as the *Nitrospira*-type NOB. The simulation results revealed that commamox could be responsible for the conversion of >10% and >20% of the influent ammonia load and nitrite respectively. Therefore, the role of commamox in the nitrogen mass balance in activated sludge systems should not be neglected and requires further investigation.

Declaration of competing interest

The authors declare that they have no known competing financial interests or personal relationships that could have appeared to influence the work reported in this paper.

Acknowledgments

The study was supported by the Polish National Science Center under project no. UMO-2017/27/B/NZ9/01039.

Appendix A. Supplementary data

Supplementary data to this article can be found online at https://doi.org/10.1016/j.jenvman.2021.113223.

Credit author statement

Mohamad-Javad Mehrani: Investigation, Software, Formal Analysis, Data Curation, Writing - Original Draft, Visualization; Xi Lu: Methodology, Software; Przemyslaw Kowal: Investigation, Formal Analysis; Dominika Sobotka: Methodology, Investigation, Formal Analysis; Jacek Makinia: Conceptualization, Methodology, Writing - Review & Editing, Supervision.

References

Annavajhala, M.K., Kapoor, V., Santo-Domingo, J., Chandran, K., 2018. Comammox functionality identified in diverse engineered biological wastewater treatment systems. Environ. Sci. Technol. Lett. 5, 110–116.
Cao, J., Zhang, T., Wu, Y., Sun, Y., Zhang, Y., Huang, B., Fu, B., Yang, E., Zhang, Q., Luo, J., 2020. Correlations of nitrogen removal and core functional genera in full-scale wastewater treatment plants: influences of different treatment processes and influent characteristics. Bioresour. Technol. 297, 122455.
Cao, Y., van Loosdrecht, M.C.M., Daigger, G.T., 2017. Mainstream partial nitritation–anammox in municipal wastewater treatment: status, bottlenecks, and further studies. Appl. Microbiol. Biotechnol. 101, 1365–1383.
Daims, H., Lebedeva, E.V., Pjevac, P., Han, P., Herbold, C., Albertsen, M., Jehmlich, N., Palatinszky, M., Vierheilig, J., Bulaev, A., Kirkegaard, R.H., von Bergen, M., Rattei, T., Bendinger, B., Nielsen, P.H., Wagner, M., 2015. Complete nitrification by Nitrospira bacteria. Nature 528, 504.
Daims, H., Lücker, S., Wagner, M., 2016. A new perspective on microbes formerly known as nitrite-oxidizing bacteria. Trends Microbiol. 24, 699–712.
Dold, P.L., Jones, R.M., Bye, C.M., 2005. Importance and measurement of decay rate when assessing nitrification kinetics. Water Sci. Technol. 52, 469–477.
Domingo-Félez, C., Smets, B.F., 2016. A consilience model to describe N2O production during biological N removal. Environ. Sci.: Water Research & Technology 2, 923–930.
Gonzalez-Martinez, A., Rodriguez-Sanchez, A., van Loosdrecht, M.C.M., Gonzalez-Lopez, J., Vahala, R., 2016. Detection of comammox bacteria in full-scale wastewater treatment bioreactors using tag-454-pyrosequencing. Environ. Sci. Pollut. Control Ser. 23, 25501–25511.
Griffin, J.S., Wells, G.F., 2017. Regional synchrony in full-scale activated sludge bioreactors due to deterministic microbial community assembly. ISME J. 11, 500–511.
Hauduc, H., Neumann, M.B., Muschalla, D., Gamerith, V., Gillot, S., Vanrolleghem, P.A., 2015. Efficiency criteria for environmental model quality assessment: a review and its application to wastewater treatment. Environ. Model. Software 68, 196–204.
Henze, M.G.W., Mino, T., van Loosdrecht, M.C.M., 2000. Activated Sludge Models ASM1, ASM2, ASM2d and ASM3. IWA Publishing, London, UK.
Hong, Y., Liao, Q., Bonhomme, C., Chebbo, G., 2019. Physically-based urban stormwater quality modelling: an efficient approach for calibration and sensitivity analysis. J. Environ. Manag. 246, 462–471.
Izadi, P., Izadi, P., Eldyasti, A., 2021. Towards mainstream deammonification: comprehensive review on potential mainstream applications and developed sidestream technologies. J. Environ. Manag. 279, 111615.
Jaramillo, F., Orchard, M., Muñoz, C., Zamorano, M., Antileo, C., 2018. Advanced strategies to improve nitrification process in sequencing batch reactors - a review. J. Environ. Manag. 218, 154–164.
Karlikanovaite-Balikci, A., Yagci, N., 2019. Determination and evaluation of kinetic parameters of activated sludge biomass from a sludge reduction system treating real sewage by respirometry testing. J. Environ. Manag. 240, 303–310.
Kits, K.D., Sedlacek, C.J., Lebedeva, E.V., Han, P., Bulaev, A., Pjevac, P., Daebeler, A., Romano, S., Albertsen, M., Stein, L.Y., Daims, H., Wagner, M., 2017. Kinetic analysis of a complete nitrifier reveals an oligotrophic lifestyle. Nature 549, 269–272.
Koch, H., van Kessel, M.A.H.J., Lücker, S., 2019. Complete nitrification: insights into the ecophysiology of comammox Nitrospira. Appl. Microbiol. Biotechnol. 103, 177–189.
Kowal, P., Mehrani, M.-J., Sobotka, D., Ciesielski, S., Stense, D., Mąkinia, J., 2021. Coexistence of Canonical Nitrifiers and Comammox Bacteria during Biomass Washout Experiments at Decreasing Solids Retention Times (in preparation).
Lawson, C.E., Lücker, S., 2018. Complete ammonia oxidation: an important control on nitrification in engineered ecosystems? Curr. Opin. Biotechnol. 50, 158–165.
Lu, X., Pereira, D.S., Al-Hazmi, T., E, H., Majtacz, J., Zhou, Q., Xie, L., Makinia, J., 2018. Model-based evaluation of N2O production pathways in the anammox-enriched granular sludge cultivated in a sequencing batch reactor. Environ. Sci. Technol. 52, 2800–2809.
Makinia, J., Rosenwinkel, K.H., Spering, V., 2006. Comparison of two model concepts for simulation of nitrogen removal at a full-scale biological nutrient removal pilot plant. J. Environ. Eng. 132, 476–487.
Makinia, J., Zaborowska, E., 2020. Mathematical Modelling and Computer Simulation of Activated Sludge Systems, second ed. IWA, UK.
Metcalf, Eddy, 2014. Wastewater Engineering: Treatment and Resource Recovery, fifth ed. McGraw-Hill, New York, United States.
Noriega-Hevia, G., Mateo, O., Maciá, A., Lardín, C., Pastor, L., Serralta, J., Bouzas, A., 2020. Experimental sulphide inhibition calibration method in nitrification processes: a case-study. J. Environ. Manag. 274, 111191.
Palomo, A., Pedersen, A.G., Fowler, S.J., Dechesne, A., Sicheritz-Pontén, T., Smets, B.F., 2018. Comparative genomics sheds light on niche differentiation and the evolutionary history of comammox Nitrospira. ISME J. 12, 1779–1793.

Park, M.-R., Park, H., Chandran, K., 2017. Molecular and kinetic characterization of planktonic Nitrospira spp. selectively enriched from activated sludge. Environ. Sci. Technol. 51, 2720–2728.
Qian, F., Wang, J., Shen, Y., Wang, Y., Wang, S., Chen, X., 2017. Achieving high performance completely autotrophic nitrogen removal in a continuous granular sludge reactor. Biochem. Eng. J. 118, 97–104.
Razavi, S., Jakeman, A., Saltelli, A., Prieur, C., Iooss, B., Borgonovo, E., Plischke, E., Lo Piano, S., Iwanaga, T., Becker, W., Tarantola, S., Guillaume, J.H.A., Jakeman, J., Gupta, H., Melillo, N., Rabitti, G., Chabridon, V., Duan, Q., Sun, X., Smith, S., Sheikholeslami, R., Hosseini, N., Asadzadeh, M., Puy, A., Kucherenko, S., Maier, H. R., 2021. The Future of Sensitivity Analysis: an essential discipline for systems modeling and policy support. Environ. Model. Software 137, 104954.
Roots, P., Wang, Y., Rosenthal, A.F., Griffin, J.S., Sabba, F., Petrovich, M., Yang, F., Kozak, J.A., Zhang, H., Wells, G.F., 2019. Comammox Nitrospira are the dominant ammonia oxidizers in a mainstream low dissolved oxygen nitrification reactor. Water Res. 157, 396–405.
Sun, Z., Liu, C., Cao, Z., Chen, W., 2018. Study on regeneration effect and mechanism of high-frequency ultrasound on biological activated carbon. Ultrason. Sonochem. 44, 86–96.
van Kessel, M.A.H.J., Speth, D.R., Albertsen, M., Nielsen, P.H., Op den Camp, H.J.M., Kartal, B., Jetten, M.S.M., Lücker, S., 2015. Complete nitrification by a single microorganism. Nature 528, 555.
Wu, Lina, Shen, Mingyu, Li, Jin, Huang, Shan, Li, Zhi, Yan, Zhibin, Peng, Yongzhen, 2019. Cooperation between partial-nitrification, complete ammonia oxidation (comammox), and anaerobic ammonia oxidation (anammox) in sludge digestion liquid for nitrogen removal. Environ. Pollut. 254.
Wu, X., Yang, Y., Wu, G., Mao, J., Zhou, T., 2016. Simulation and optimization of a coking wastewater biological treatment process by activated sludge models (ASM). J. Environ. Manag. 165, 235–242.
Yu, L., Chen, S., Chen, W., Wu, J., 2020. Experimental investigation and mathematical modeling of the competition among the fast-growing "r-strategists" and the slow-growing "K-strategists" ammonium-oxidizing bacteria and nitrite-oxidizing bacteria in nitrification. Sci. Total Environ. 702, 135049.
Zhang, D., Su, H., Antwi, P., Xiao, L., Liu, Z., Li, J., 2019. High-rate partial-nitritation and efficient nitrifying bacteria enrichment/out-selection via pH-DO controls: efficiency, kinetics, and microbial community dynamics. Sci. Total Environ. 692, 741–755.
Zhou, X., Liu, X., Huang, S., Cui, B., Liu, Z., Yang, Q., 2018. Total inorganic nitrogen removal during the partial/complete nitrification for treating domestic wastewater: removal pathways and main influencing factors. Bioresour. Technol. 256, 285–294.
Zhu, A., Guo, J., Ni, B.-J., Wang, S., Yang, Q., Peng, Y., 2015. A novel protocol for model calibration in biological wastewater treatment. Sci. Rep. 5, 8493.